Journal of Nuclear Materials 386–388 (2009) 1056–1059

Contents lists available at ScienceDirect

Journal of Nuclear Materials

journal homepage: www.elsevier.com/locate/jnucmat

Compatibility between Be–V Alloy and F82H steel

K. Tsuchiya *, Y. Namekawa, T. Ishida

Neutron Irradiation and Testing Reactor Center, Japan Atomic Energy Agency (JAEA), 4002, Narita-cho, Oarai-machi, Higashiibaraki-gun, Ibaraki-ken 311-1393, Japan

ARTICLE INFO

PACS:
81.56.Jt
82.56.Lz

ABSTRACT

Beryllium alloys such as Be–Ti and Be–V are promising candidates for advanced neutron multipliers from viewpoints of high melting point, high beryllium content, low radio-activation, and good chemical stability. In this study, the compatibility between structural material F82H steel and Be–7 at.%V that includes αBe phase was investigated. After annealing, reaction products at the surface of F82H steel and Be–7 at.%V specimen were analyzed by X-ray diffraction analysis and EPMA/SEM analysis. The thickness and rate constant of reaction layer at the surface of F82H steel were evaluated and good compatibility between Be–V and F82H was clearly observed.

1. Introduction

Beryllium (Be) metal is a reference material in the blanket design [1]. However, it may not be applicable to the DEMO blanket that requires high temperature (~900 °C) and high neutron dose (~20000 appm He, ~50 dpa). Therefore, it is necessary to develop an advanced material that has high temperature resistance and high radiation resistance. Beryllides such as $Be_{12}Ti$ and $Be_{12}V$ have been proposed as promising candidates for advanced neutron multipliers from the viewpoints of high melting point, high beryllium content, fast decay of gamma dose rate and good chemical stability [2–5].

In previous studies, compatibility of Be metal and Be–Ti alloys with F82H steel was evaluated [6,7], where F82H is a candidate structural material for fusion reactors. In the results, the thickness of the reaction layer between Be–Ti and F82H was smaller than that between Be and F82H. The melting point of Be–V is higher than that of Be–Ti. Therefore, better properties may be expected for Be–V alloys than for Be–Ti alloys. However, compatibility of Be–V alloys with F82H has not been evaluated so far.

In the present study, the compatibility between Be–7 at.%V alloy and F82H was investigated; this alloy has better ductility than stoichiometric $Be_{12}V$.

2. Experimental

2.1. Specimens

Be–V (Be–7 at.%V) specimens were fabricated from beryllium and vanadium powders by an arc melting process. The specimens were machined to disks which have approximately 8 mm in diameter and 1.5 mm in thickness, and were mirror-polished on the surface. The Be–V specimens were prepared by NGK Insulators Ltd. The chemical compositions of the Be–V specimen are shown in Table 1. The content of BeO in these specimens was about 0.60 wt% at maximum. The surface of the Be–V specimen was ultrasonically cleaned with acetone. Fig. 1 shows the backscattered electron image and element distribution for a Be–7 at.%V specimen.

The chemical composition of the F82H specimens is also shown in Table 1. The dimension of the F82H specimens was 10 mm in diameter and 2 mm in thickness. The F82H specimens were also mirror-polished and ultrasonically cleaned with acetone.

2.2. Procedure in compatibility tests

Fig. 2 shows the configuration of the capsule for annealing tests. Diffusion couples for the compatibility tests consisted of Be–7 at.%V and F82H, and were filled with pure helium gas and sealed by welding. Compatibility tests were carried out at 600, 700 and 800 °C by annealing the diffusion couples in an electric furnace under vacuum conditions. Annealing times were 100, 300 and 710 h. After annealing, the interaction in the diffusion couple was studied as follows.

The contact surface of each specimen was observed by optical microscopy. X-ray diffractometry (XRD) was performed to identify the reaction products in the near surface region. The microstructure and thickness of the reaction layer were analyzed in the cross section by scanning electron microscopy (SEM). The composition of the layer was identified by electron probe microanalysis (EPMA).

3. Results and discussion

3.1. Identification of reaction products

After the annealing of the specimens, marks of the chemical interaction were investigated visually. It was observed that the

* Corresponding author. Tel.: +81 29 266 7041; fax: +81 29 266 7073.
E-mail address: tsuchiya.kunihiko@jaea.go.jp (K. Tsuchiya).

0022-3115/$ - see front matter © 2008 Elsevier B.V. All rights reserved.
doi:10.1016/j.jnucmat.2008.12.273

Table 1
Chemical compositions of the specimens used in compatibility tests.

Material (wt%)	Elements							
	Be	V	BeO	Mg	Al	Si	Fe	Co
Be–7 at.%V	71.5	28.7	0.61	0.001	0.059	0.038	0.007	<0.01
	Elements							
	Fe	Cr	Ni	W	Mn	Al	V	C
F82H	Bal.	7.78	0.02	1.98	0.1	0.001	0.07	0.09

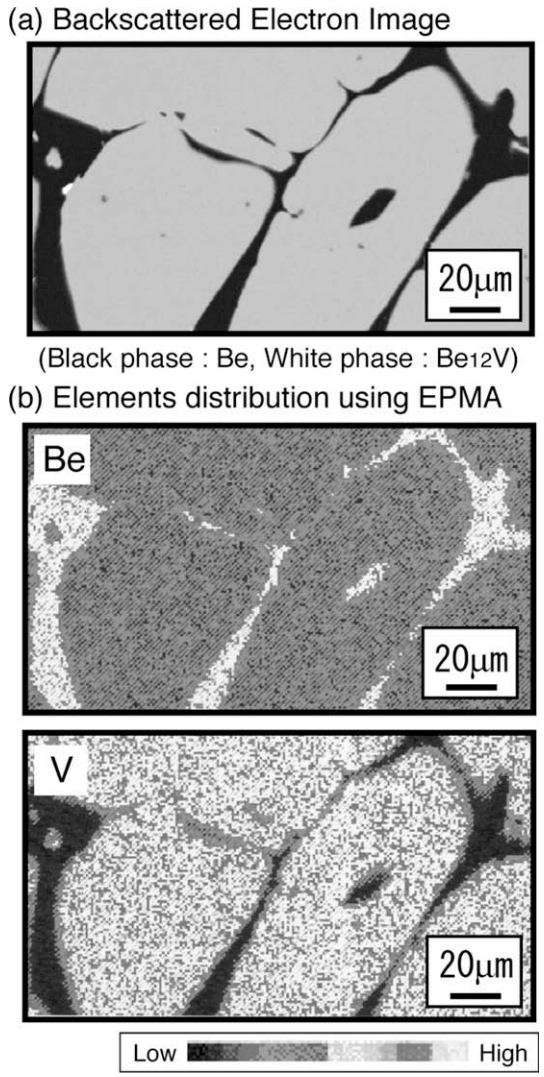

Fig. 1. Backscattered electron image and element distribution for a Be–7 at.%V specimen.

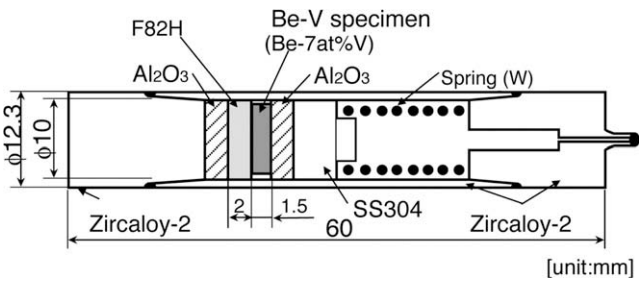

Fig. 2. Configuration of the capsule for annealing tests.

reaction areas of the contact surfaces of Be–7 at.%V/F82H increased with increasing the annealing temperature and time.

Results of XRD on the surface of Be–7 at.%V alloy and F82H at 600 and 800 °C during 710 h are shown in Fig. 3. On the Be–V specimen, no reaction products were found by XRD after annealing at 600 °C. At 800 °C, however, Be_2V and $Be_{12}V$ were detected by XRD at the surface of Be–7 at.%V. As for the F82H specimen in contact with Be–V, reaction products found at the surface were analyzed by XRD, and Be_2Fe was identified as a reaction product.

3.2. SEM/EPMA analyses of specimens

Quantitative point analyses on F82H were performed by EPMA for the typical phases observed by SEM, and Fig. 4 shows results of the analyses at the cross section of F82H and Be–V alloy. Vanadium was not detected in the reaction layer or in the F82H base metal.

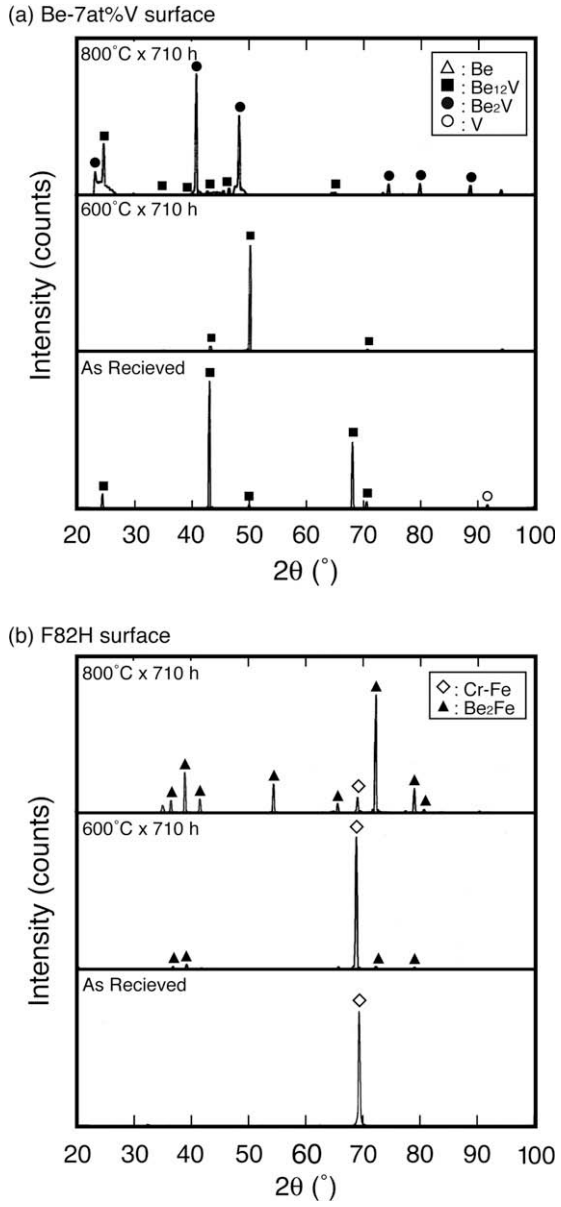

Fig. 3. XRD profiles at the surfaces of Be–7 at.%V and F82H specimens after annealing tests for 710 h.

3.2.1. Be–V surface

The reaction layers of interaction were not found by SEM observation at the surface of each Be–V specimen for the couple of Be–7 at.%V/F82H after annealing at 600 and 700 °C. However, a reaction layer and a layer with deficiency of Be were observed after annealing at 800 °C as shown in Fig. 4. Thickness of the reaction layer at the Be–V surface of the Be–7 at.%V/F82H couple was about 10 μm. The contents of Be and V in the reaction layer were about 70 and 30 at.%, respectively. It is considered that the phase in the reaction layer was almost composed of Be_2V phase. Thickness of the deficiency area at the Be–V surface was about 150 μm.

3.2.2. F82H surface

In contract, a thin reaction layer was found even at 600 °C at the F82H specimen of the Be–7 at.%V/F82H couple. Furthermore, one reaction layer and one diffusion layer were observed at the surface of each F82H specimen after annealing at 700 and 800 °C, as shown in Fig. 4.

Thickness of the reaction layer at the F82H surface was about 40 μm after annealing at 800 °C. The contents of Be and Fe in the reaction layer were about 28 and 64 at.%, respectively. Therefore, it is considered that this phase in the reaction layer was almost composed of Be_2Fe phase.

As for the diffusion layer at the F82H surface, the thickness was about 150 μm. Three phases existed in the diffusion layer as seen in Fig. 4; gray phases (D7-3, D7-4) and white phases (D7-5) in the diffusion layer were supposed to be Fe–Cr and Fe–W phases, respectively. It is considered that small black particles were a mixture of Be, Be_2Fe and Fe–Cr phases.

3.3. Thickness and rate constant of reaction layer on F82H surface

Thickness of reaction layer (d) generated to the diffusion area at a constant temperature is represented by the following equation:

$$d = k \cdot t^n, \tag{1}$$

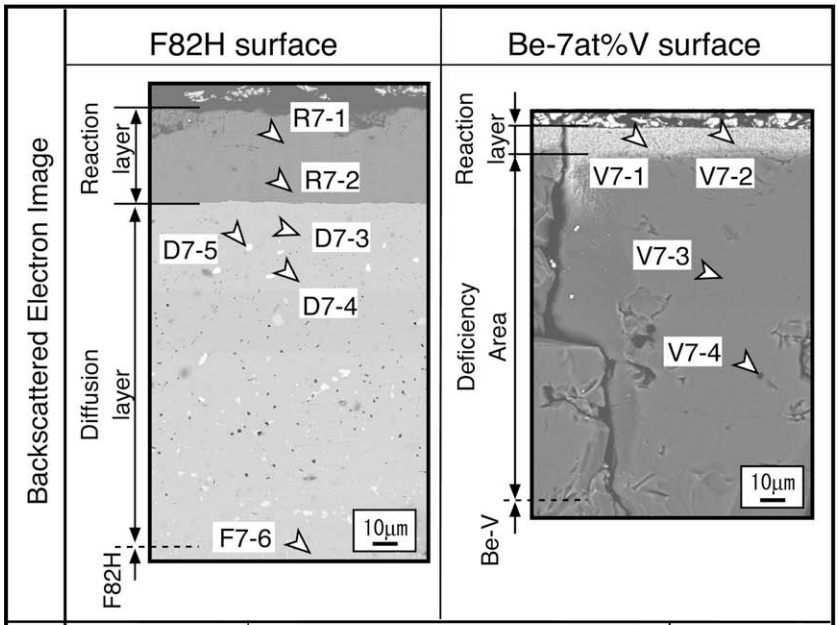

	Measuring point		Composition (at%) Be	V	Fe	Cr	W	Estimated compound
F82H	Reaction layer	R7-1	26.9	0.1	64.6	5.4	2.6	Be_2Fe (Dark Gray)
		R7-2	28.3	0.1	63.6	5.1	2.9	
	Diffusion layer	D7-3	13.8	0.2	78.6	7.2	0.2	Fe-Cr (Be_2Fe) (Gray)
		D7-4	10.8	0.2	81.6	7.3	0.1	
		D7-5	2.0	0.0	36.6	3.1	58.3	(Fe-W) (White)
	Base metal *	F7-6	0.0	0.3	91.1	8.0	0.5	Fe-Cr
Be-7at%V	Reaction layer	V7-1	67.4	31.1	0.0	1.2	0.0	Be_2V (White)
		V7-2	70.8	28.4	0.0	0.5	0.0	
	Deficiency Area	V7-3	92.3	6.7	0.0	1.0	0.0	$Be_{12}V$ (Gray)
		V7-4	99.9	0.1	0.0	0.0	0.0	Be (White)

* : no attacked area

Fig. 4. Result of quantitative EPMA analyses at the surfaces of F82H and Be–7 at.%V after annealing at 800 °C for 710 h.

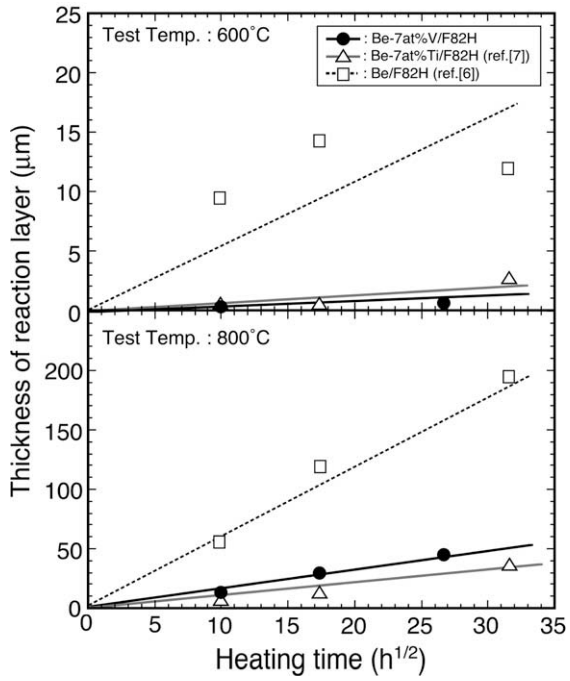

Fig. 5. Change in thickness of the reaction layer at the surface of F82H with annealing time in compatibility tests between Be–7 at.%V and F82H.

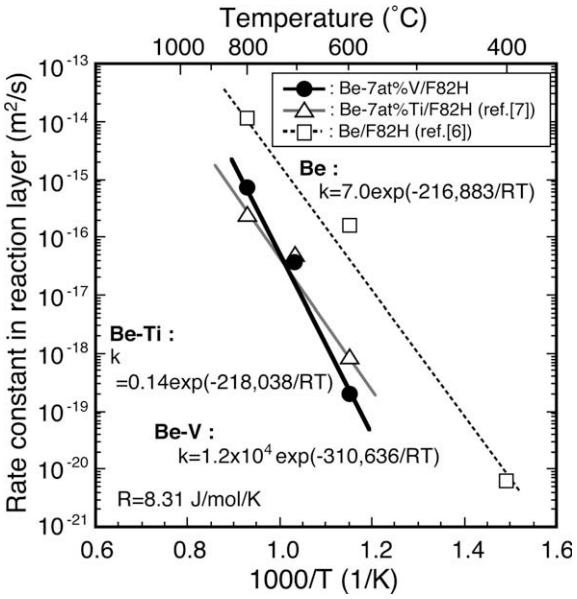

Fig. 6. Rate constant in reaction layer at F82H surface of Be–7 at.%V/F82H.

where k, t and n represent the rate constant of reaction layer, the reaction time and the index number of reaction time, respectively. Generally, the growth of reaction layer is controlled by diffusion phenomena and n is 1/2 [8].

Fig. 5 shows results of thickness measurements of the reaction layer at F82H surface of Be–7 at.%V/F82H. Results for beryllium [6] and Be–7 at.%Ti [7] with F82H are also shown in this figure. The thickness of the reaction layer between Be–7 at.%V and F82H after annealing at 600 °C for 710 h was less than 1 μm, whereas the reaction layer for beryllium metal was about 15 μm thick at 600 °C for 1000 h. Similarly, at 800 °C for 710 h, the thickness of the reaction layer for Be–7 at.%V was less than 50 μm, whereas that of beryllium metal was about 200 μm at 800 °C for 1000 h. It is also noted that thickness of the reaction layer between Be–7 at.%V and F82 H was almost the same as that between Be–7 at.%Ti and F82H. Thus, it is clear that the compatibility between Be–V and F82H was almost equivalent to that between Be–Ti and F82H and much better than that between Be and F82H.

The rate constant of the reaction layer evaluated as in Ref. [9] is shown in Fig. 6 as a function of the reciprocal temperature. The maximum temperature of beryllium region in the blanket is assessed to be 500 °C in the point of the swelling limitation [10]. On the other hand, temperature of beryllium region is assessed to be 600 °C in the point of chemical stability such as steam interaction [11]. The limited temperature of beryllium region is fixed in the fusion blanket. Thus, compatibility was evaluated at 500 °C in this study. The rate constant for Be metal was about 2×10^{-18} m^2/s at 500 °C, and this rate constant was the same as that for Be–V at about 650 °C. On the other hand, the Arrhenius equations are represented in Fig. 6 and each activation energy (E) was obtained. The activation energy for Be–V in the present study was about 310kJ/mol and this value was larger than that of Be–Ti or Be (E = ~210 kJ/mol).

4. Conclusions

The compatibility between Be–V alloy (V content: 7 at.%) and F82H was studied by annealing at 600, 700 and 800 °C, and the Be–V alloy showed advantages over Be. Deficiency of Be and reaction product (Be_2V) was observed at the Be–V surface after annealing at 800 °C. The gray phase in the reaction layer at the F82H surface was found to be composed of Be_2Fe. The thickness of the reaction layer at the F82H surface was smaller than that between Be metal and F82H. Good compatibility between Be–V and F82H was clearly observed and it is considered that the Be–7 at.%V can be used up to about 650 °C in the point of compatibility with F82H steel.

Acknowledgments

The authors are grateful to Dr K. Hayashi of JAEA for his helpful advice for preparation of the manuscript of the paper.

References

[1] H. Kawamura, M. Okamoto (Eds.), in: Proceedings of the Third IEA International Workshop on Beryllium Technology for Fusion, 22–24 October 1997, Mito, Japan, JAERI-Conf 98-001.
[2] H. Kawamura, H. Takahashi, N. Yoshida, V. Shestakov, Y. Ito, M. Uchida, H. Yamada, M. Nakamichi, E. Ishitsuka, Fus. Eng. Des. 61&62 (2002) 391.
[3] H. Kawamura, E. Ishitsuka, K. Tsuchiya, M. Nakamichi, M. Uchida, H. Yamada, K. Nakamura, H. Ito, T. Nakazawa, H. Takahashi, S. Tanaka, N. Yoshida, S. Kato, Y. Ito, Nucl. Fus. 43 (2003) 675.
[4] H. Kawamura, H. Takahashi, N. Yoshida, Y. Mishima, K. Ishida, T. Iwadachi, A. Cardella, J.G. van der Laan, M. Uchida, K. Munakata, Y. Sato, V. Shestakov, S. Tanaka, J. Nucl. Mater. 329–333 (2004) 112.
[5] K. Tsuchiya, T. Hoshino, H. Kawamura, Y. Mishima, N. Yoshida, T. Terai, S. Tanaka, K. Munakata, S. Kato, M. Uchida, M. Nakamichi, H. Yamada, D. Yamaki, K. Hayashi, Nucl. Fus. 47 (2007) 1300.
[6] H. Kawamura, M. Kato, E. Ishitsuka, S. Hamada, K. Nishida, M. Saito, Fus. Eng. Des. 29 (1995) 475.
[7] K. Tsuchiya, H. Kawamura, T. Ishida, J. Nucl. Mater. 367–370 (2007) 1018.
[8] O. Taguchi, KINZOKU (Mater. Sci. Technol.) 74 (2004) 911.
[9] V. McGahay, J. Non-Cryst. Solids 349 (2004) 234.
[10] M.C. Billone, C.C. Lin, D.L. Baldwin, Fus. Technol. 19 (1991) 1707.
[11] R.A. Anderl, K.A. Mccarthy, M.A. Oates, D.A. Petti, R.J. Pawelko, G.R. Smolik, J. Nucl. Mater. 258–263 (1998) 750.